THERMAL CRACK ANLYSIS BASED ON PRACTICAL 3-D FEM ANALYSIS MODEL

(Translation from Proceedings of JSCE, No.550/V-33, November 1996)

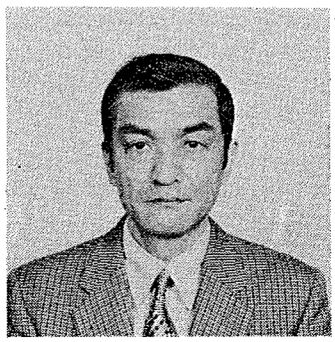

Hiroaki MORIMOTO

Wataru KOYANAGI

This paper deals with a practical 3-D analysis model for thermal stress and crack width. The model applied in this study is based on the concept of discrete crack approach. The authors analyzed the thermal stress and crack width in a wall structure by FEM incorporating the 3-D analysis model, and elucidated the 3-D distribution of thermal stress and crack width in walls in comparison with the actual measurements. The effect of reinforcement on crack control was also investigated. Applicability and problems of the 2-D FEM analysis and the extended CP method were studied as well.

Keywords: thermal crack, discrete crack model, bond slip model, 3-D FEM, extended CP method, crack control, thermal stress

Hiroaki Morimoto is a Professor in the Department of Civil Engineering at Gifu University, Gifu, Japan. He obtained his Doctor of Engineering Degree in 1989 from Kyoto University. His research interests include thermal stress of mass concrete, and creep and relaxation of young age concrete. He is a member of JSCE and JCI.

Wataru Koyanagi is a Professor in the Department of Civil Engineering at Gifu University, Gifu, Japan. He obtained his Doctor of Engineering Degree in 1977 from Kyoto University. His research interests cover behavior of concrete material, reinforced concrete members and structures, structural design methods and the application of new building materials. He is a member of JSCE, JCI, JSMS and ACI.

1. INTRODUCTION

In the stages of design and construction, sufficient care should be exercised to avoid thermal cracking of concrete as it adversely affects the durability and functionality of structures. When taking measures against cracking, the relationship between the conditions of the measures, crack width and other factors should be examined in advance. In addition to previously proposed methods of analyzing thermal cracking, two methods have been proposed by the Japan Concrete Institute Committee on Thermal Stress of Massive Concrete (hereafter referred to as the "JCI Mass Concrete Committee") in recent years. These are the extended CP method[1] and the finite element method (FEM) thermal crack analysis model[1]. Most of the crack analysis techniques proposed so far model cracks two-dimensionally, even though actual cracks are considered to develop three-dimensionally. Conventional two-dimensional techniques are therefore equivocal as to the stress and crack width changes in the direction of depth. In two-dimensional FEM thermal crack analysis (hereafter referred to as "2-D analysis"), the treatment of temperature distribution along the wall thickness also poses a problem. In practical terms, the conditions of measures to prevent thermal cracks are determined empirically, which could lead to unsatisfactory results. In order to realize effective control of thermal cracking, the relationship between the measures and their crack-inhibiting effects should be grasped three-dimensionally. Three-dimensional thermal crack analysis (hereafter referred to as "3-D analysis") is also significant as a means to verify and improve the accuracy of such simple calculation methods as the extended CP method and 2-D analysis.

In this study, the authors analyzed the thermal stress and crack width in a wall structure by the 3-D analysis method incorporating the discrete crack approach, and elucidated the 3-D distribution of thermal crack width in walls in comparison with the actual measurements. The 3-D analysis results were also compared with the results of 2-D analysis and the extended CP methods, with their applicability and problems being pointed out. The 3-D analysis method proposed in this study was also used to elucidate the crack width controlling effect of reinforcement.

2. THREE-DIMENSIONAL ANALYSIS MODEL

The 3-D analysis model applied in this study is based on the concept of the JCI Mass Concrete Committee model[1] using the discrete crack approach. As shown in Fig. 1, this model expresses a crack as a gap between two nodes defined at the position of cracking.

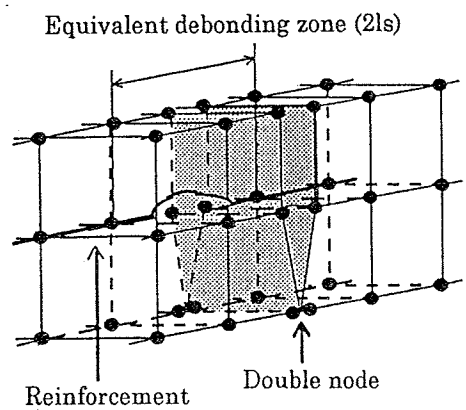

Fig. 1 3-D Analysis Model

In this study, two nodes are defined at points where a crack is expected to occur (hereafter referred to as "double nodes"). Double nodes are combined with joint elements with a high rigidity until the onset of cracking. At the crack onset, the rigidity of the binding elements is minimized to express the occurrence of cracking. The bond slip of reinforcement is modeled by assuming a zone with no bond at all from the crack faces to a defined distance. This bondless zone is defined as an equivalent debonding zone, ls. Elastic constitutional laws are used for concrete and reinforcement.

3. CRACK ANALYSIS PROCEDURE BY FEM

A 3-D analysis was conducted by the FEM incorporating the analysis model shown in Fig. 1. In the 2-D analysis, a model made by two-dimensionalizing the 3-D model shown in Fig. 1 was used. The crack analysis procedures[2],[3] are as follows:

(1) Model several positions where a crack is expected as shown in Fig. 1. Link double nodes with joint elements having extremely high rigidity.

(2) Proceed with thermal stress calculation incrementally.

(3) Compare the thermal stress around double nodes with the tensile strength at each time step. When the thermal stress exceeds the tensile strength, minimize the rigidity of the joint elements to express cracking.

(4) Calculate the redistribution of stress resulting from the cracking, and determine the stress and deformation after cracking. Calculate the crack width as a difference in the displacements of the two nodes of a double node.

(5) When the stress distribution leads to crack development or new cracking, repeat the processes of (3) and (4).

4. EXTENDED CP METHOD

The extended CP method was proposed by the JCI Mass Concrete Committee to calculate thermal crack width, and is an extension of the CP method, which is used to calculate thermal stress. This method begins by calculating the strain increment of reinforcement at the crack onset from the equilibrium conditions of forces and compatibility conditions of deformation in the zone where the stress is released when cracking occurs (defined as "stress release zone," lc). The final strain increment is then determined taking into account the equilibrium and deformation of the entire structure. The crack width is then calculated by multiplying the reinforcement strain by the equivalent debonding zone, ls (the same concept as the FEM analysis model).

5. OUTLINE OF ANALYSIS

5.1 structure under analysis

The structure under analysis[4] is a wall 1.0 m in width, 1.5 m in height, and 15 m in length; on a concrete base 5.0 m in width, 1.5 m in height, and 15.3 m in length as shown in Fig. 2. D19 distributing bars are placed longitudinally at a reinforcement ratio of 0.27%. The mix proportions of the wall and base concretes are given in Table 1. Normal portland cement was used for the concretes. The placing temperature was 15℃. The wall is fitted with effective concrete stress gauges, reinforcement strain gauges, crack gauges, thermocouples, and stress-free strain gauges at different points, to measure

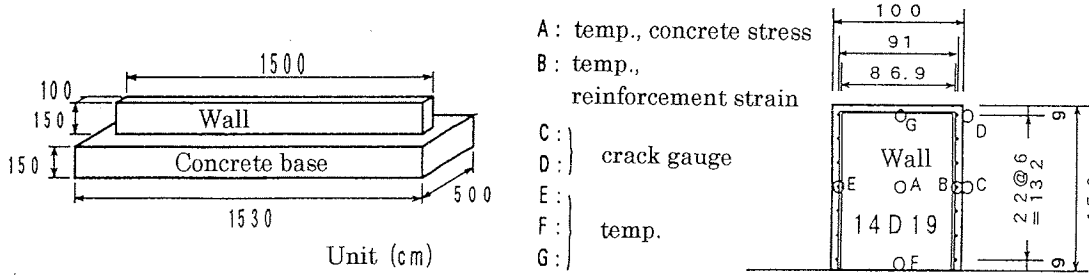

Fig.2 Structure under Analysis

Table 1 Mix Proportion of Concrete

	G_{max} (mm)	Slump (cm)	Air (%)	W/C (%)	s/a (%)	Unit content (kg/m³)				
						W	C	S	G	Ad
Base	25	8±2.5	4±1.0	55.0	42.0	153	278	785	1118	0.556
Wall	25	8±2.5	4±1.0	50.0	43.0	160	320	777	1063	0.640

Ad: Air entraining and water reducing agent

Table 2 Properties of wall concrete

Slump (cm)	Air (%)	Temp. of fresh concrete (℃)	Thermal expansion coefficient ($\times 10^{-6}$/℃)	Item	Age(days)		
					3	7	28
8.9	4.1	15.0	5.46	Compressive strength (kgf/cm²)	129	183	285
			(8.45)*	Elastic modulus ($\times 10^5$kgf/cm²)	1.52	2.17	3.01

*: value obtained from measurement of wall

the concrete stress , reinforcement stress, crack width, temperature, and thermal expansion coefficient. Figure 2 shows typical measuring points. Strength tests on the concretes were also conducted separately, and the thermal expansion coefficient was measured using beams 10 by 10 by 40 cm in which strain gauges and thermocouples were embedded. These results are given in Table 2. The thermal expansion coefficients measured by stress-free strain gauges are also given in the table. It should be noted that a crack across the height of the wall occurred near mid-length at the age of 7 days.

5.2 Analysis method

a) Temperature analysis
The temperature of a wall section was analyzed by the 2-D FEM. The following equation was selected for the adiabatic temperature rise of concrete, Q (℃), as it derives values closest to the actual values:

$$Q(t) = 57.9\left\{1 - \exp\left(-0.716t\right)\right\} \qquad (1)$$

where t = age (days)

b) Crack analysis by FEM
The elements were meshed so as to coincide with the distributing bars, as the reinforcing bars were modeled by bar elements. The bond with the concrete base at the bottom of the wall was assumed to be perfect so that no separation occurred even after cracking. The compressive strength, fc (kgf/cm^2), tensile strength, ft (kgf/cm^2), and elastic modulus, E (kgf/cm^2), were evaluated by the following equations calculated from the measurements given in Table 2.

$$f_c'(t) = \frac{t}{0.01585 + 0.0025t} \qquad (2)$$

$$f_t(t) = \frac{t}{0.1408 + 0.0343t} \qquad (3)$$

$$E(t) = \frac{t}{1.137 \times 10^{-5} + 2.914 \times 10^{-6} t} \qquad (4)$$

where t = age (days)

The effects of concrete relaxation were taken into account approximately using the so-called "effective elastic modulus" obtained by multiplying the value of Eq. (2) by the elastic modulus reduction rate[5] shown in Fig. 3. The measurements by stress-free strain gauges were used as the thermal expansion coefficient of concrete. The occurrence of a crack was assumed when the thermal stress exceeded 80% of the tensile strength, in consideration of the rate of increase in the thermal stress, fluctuation of strength of actual structures, and existing study results[6]. The above-mentioned temperature analysis results were used as the temperature history at each element during the crack analysis (hereafter referred to as "temperature data"). In the 3-D analysis, the temperature changes longitudinally were approximately neglected, and the 2-D temperature data of a wall section was applied. On the other hand, the thermal analysis results cannot be used as the temperature data as such in the 2-D analysis, as the section under thermal analysis is different from the section under crack analysis (they are perpendicular to each other). For this reason, average or mid-thickness temperatures of the section are generally used. In either case, however, the temperature fluctuations along the wall thickness cannot be taken into account; and it has been pointed out that this is one of the limitations of the 2-D analysis. In this study, the two above-mentioned methods were adopted to treat the temperature data for the 2-D analysis, and a plane stress field was also assumed. The analyses in which average temperature and mid-thickness temperatures were used are hereafter referred to as Case A and Case B,

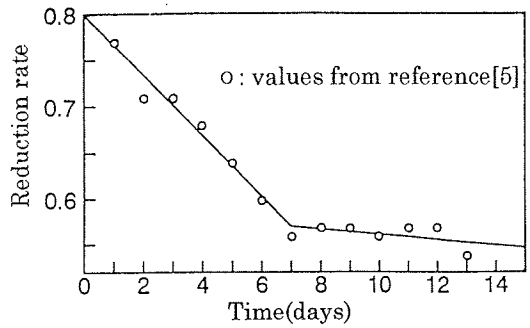

Fig. 3 Reduction Rate of Elastic Modulus

respectively. In consideration of the values recommended by the JCI Mass Concrete Committee, the equivalent debonding zone, ls, in the 2-D analysis model was assumed to be 15 cm.

c) Extended CP method

Analysis by extended CP method was conducted on a personal computer program[7] devised by the JCI Mass Concrete Committee. In consideration of the committee proposals, the stress release zone, lc, and equivalent debonding zone, ls, were assumed to be 165 cm and 15 cm, respectively. The mechanical properties of concrete used for the analysis were the same as those used in the FEM analysis.

5.3 Items of investigation

a) Effects of ls on the calculation results

The selection of an appropriate equivalent debonding zone to express bond slip is critical in the analysis model shown in Fig. 1. Whereas the JCI Mass Concrete Committee recommends specific values of ls for the extended CP method and 2-D analysis models, no reference is made by the committee regarding the ls values for the 3-D analysis models. Accordingly, the authors investigated the effects of ls from the 3-D models on the calculation results, as well as appropriate values for ls. Analysis was carried out for four values of ls: 5, 10, 15, and 20 cm.

b) 3-D distribution of thermal crack width in the wall

Thermal crack width is considered to change in both the directions of wall height and thickness. However, it is difficult to accurately analyze such 3-D changes by 2-D analysis or extended CP methods. The authors therefore investigated the 3-D distribution of thermal crack width, reinforcement and thermal stresses in the wall by 3-D analysis. Accuracy of the 3-D analyses was then verified by comparison with the actual measurements.

c) Applicability of 2-D analysis and extended CP method

As previously stated, the fluctuations in temperature along the wall depth is generally disregarded in the 2-D analyses of walls. Therefore the effects of internal restraining stress on crack width tends to be unclear. On the other hand, the extended CP method can take account of the temperature distribution, but cannot analyze the changes in the crack width along the wall's depth. The applicability of 2-D analysis and extended CP methods is discussed in comparison with 3-D analysis.

d) Crack width controlling effect of reinforcement

Placing the so-called "crack controlling bars", or bars perpendicular to cracks, is effective as a means of controlling the crack width[8]. It is necessary to investigate the crack-controlling effect of reinforcement, in order to determine its optimum content. In this study, to elucidate the relationship between the reinforcement content and the crack width reinforcement ratios of 0.27%, 0.6%, and 0.9% were adopted for the 3-D analyses.

6. ANALYSIS RESULTS

6.1 Temperature rise in the wall

Figure 4 shows the measured and calculated temperatures at mid-thickness and on the surface (Points A and B in Fig. 2) of the wall's mid-height. The measurements show that the concrete temperature at mid-thickness hits a peak of 46℃ at 2 days. This shows a rise of 31℃ from the placing temperature. The peak surface temperature is 38℃. The differences between the mid-thickness and surface temperatures is widest at around 3 days at 13℃. The calculated values generally shows congruence with the experimental results. The largest incongruency is 5℃. The temperature rise in the wall after 9 days is considered to be due to a rise in the ambient temperature.

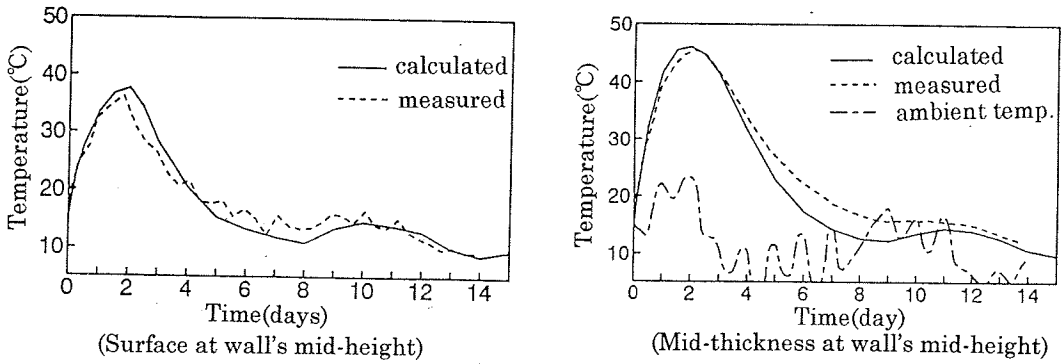

Fig. 4 Concrete Temperature

6.2 Effect of equivalent debonding zone

a) Crack width

Figures 5 to 8 show the measured crack width on the surface (Point C in Fig. 2) at the mid-height of the wall, as well as the calculated values; with the ls values being 5, 10, 15, and 20 cm. The measured crack width immediately after occurrence was around 0.27 mm. Crack width tended to increase slightly with an increase in age, reaching 0.37 mm at 14 days. According to the analysis, cracking occurred at 5 days in all cases, and the crack width tended to increase slightly thereafter, similar to actual measurements. The temporary reduction in the calculated crack width at around 11 days is due to a fluctuation in the ambient temperature. The larger crack width at mid-thickness compared to that near the surface is due to a higher tensile stress occurring at mid-thickness. Therefore, when a crack is identified on a wall surface, the probability of its continuing through may be significantly high. As ls expresses the bond slip, a large ls means that a large bond slip zone is assumed. The figures shows that a large value of ls leads to a large crack width by calculation. Figure 9 shows the relationship between the calculated crack width and the ls values at 14 days. The figure reveals that a larger value of ls leads to a larger calculated crack width at both positions. This indicates that a larger bond slip zone leads to a larger crack width. A larger values of ls also leads to smaller differences in mid-thickness and on surface crack widths. This is because the crack-restraining effect of reinforcement decreases as ls increases. When comparing the calculated and measured crack widths on the surfaces at the wall's mid-height in Figures 5 to 8, with ls being 15 cm and 20 cm, the calculated maximum crack widths agree well with the measured value of 0.37 mm. On

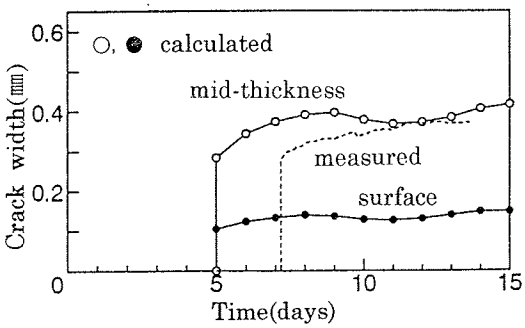

Fig. 5 Development of Crack Width(ls=5 cm)
(Mid-height of the wall)

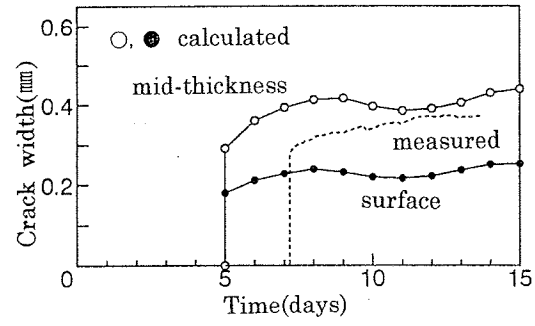

Fig. 6 Development of Crack Width(ls=10 cm)
(Mid-height of the wall)

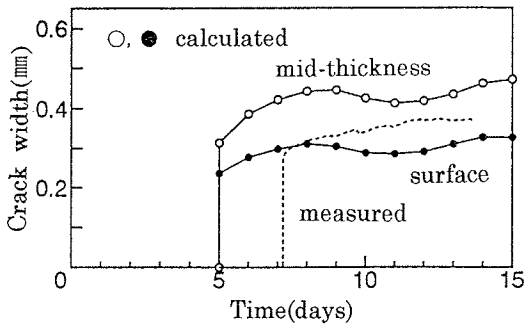

Fig. 7 Development of Crack Width(ls=15 cm)
(Mid-height of the wall)

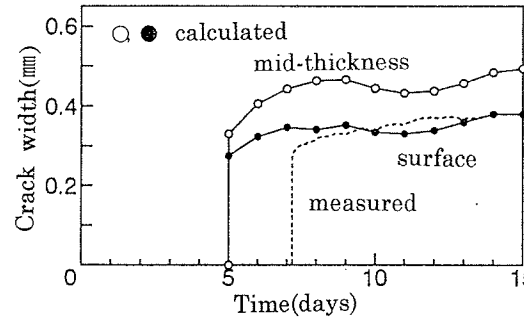

Fig. 8 Development of Crack Width(ls=20 cm)
(Mid-height of the wall)

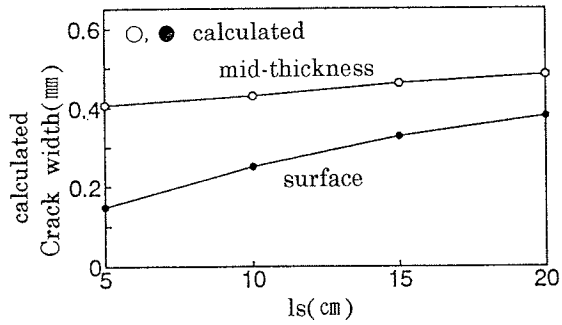

Fig. 9 Changes of Crack Width due to the Value of ls
(Mid-height of the wall)

the other hand, calculated maximum crack widths with ls being 5 cm and 10 cm are only 40% and 60%, respectively, of the measured value, and are excessively small as estimations of crack widths. Consequently, 15 to 20 cm are considered to be appropriate ls values for the 3-D analysis models. These values nearly coincide with the recommended ls, 20 cm, for the extended CP method.

b) Reinforcement stress

Figures 10 to 13 show the measured reinforcement stress at the wall's mid-height crack position(Point B in Fig. 2) and calculated reinforcement stress for each ls value. The figures indicate a tendency of reinforcement stress history similar to that of crack width. The calculated reinforcement stress decreases as the ls value increases. This is because a larger values of ls leads to a lower average strain of reinforcement in the equivalent debonding zone. The measured reinforcement stress at 8 days is approximately 2100 kgf/cm^2. The calculated reinforcement stress with ls being 15 cm is approximately 2150 kgf/cm^2, agreeing well with the actual measurements. The calculated values with ls at 20 cm also agrees well with actual measurements. Accordingly, the ls values of 15 to 20 cm are also found to lead to good calculation results in regard to reinforcement stress.

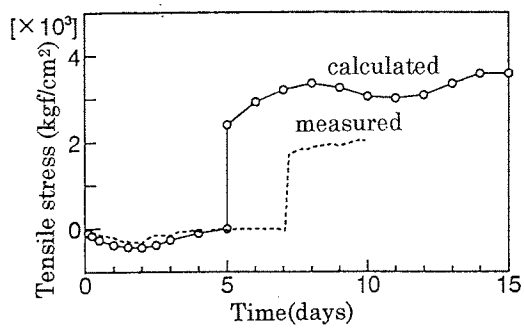

Fig. 10 Development of Reinforcement Stress (ls=5 cm)

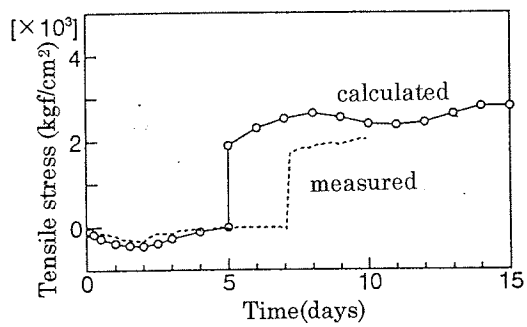

Fig. 11 Development of Reinforcement Stress (ls=10 cm)

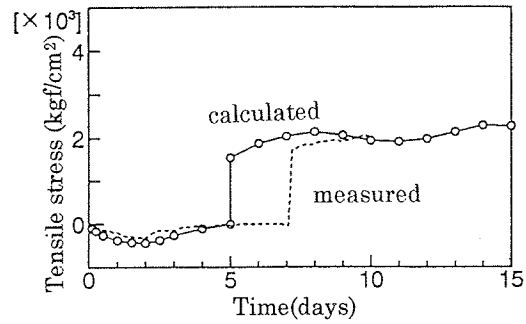

Fig. 12 Development of Reinforcement Stress (ls=15 cm)

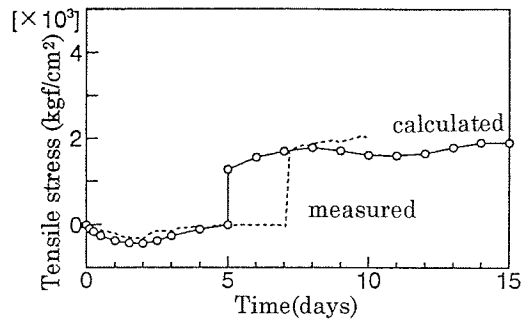

Fig. 13 Development of Reinforcement Stress (ls=20 cm)

c) Concrete stress

Figure 14 shows the measured concrete stress at a section of the wall's mid-height approximately 2 m away from the crack (Point A in Fig. 2) and the corresponding values calculated with ls being 15 cm. The calculated values at mid-thickness and on the surface are shown. From the figure, calculated stress slightly exceeds the measured stress in regard to compressive stress at early ages. However, calculated and measured stress agree well regarding the tensile stress that gradually develops with a drop in wall temperature. Stress released due to cracking is observed in the calculated surface stress at 5 days. No marked effect of ls on the concrete stress was observed.

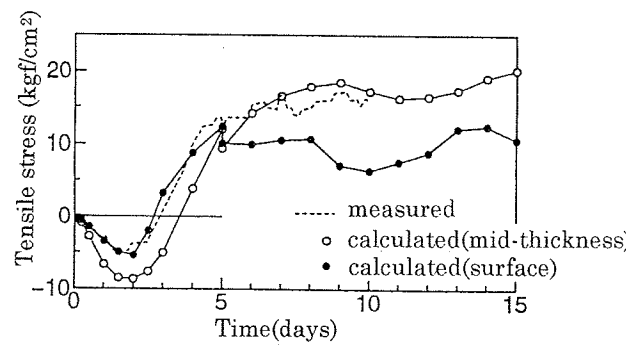

Fig. 14 Development of Concrete Stress (ls=15 cm)

6.3 3-D distribution of thermal stress and crack width

Figure 15 displays the 3-D distribution of concrete stress of a section at approximately 2 m from the crack with ls being 15 cm. The diagrams are air views of the wall from upper right, and provide a sound grasp of the stress distribution in the wall. The distribution contour of the section, resulting from the combined internal and externally restrained stresses, changes from concave to convex with an increase in age. Figure 16 shows the crack width with ls being 15 cm. The figure provides a sound visual grasp of the crack distribution. The crack width distribution is expressed as a contour convex towards upper center having its peak at mid-thickness near the top of the wall. In other words, the crack width in the center is larger than on the surfaces. The contour of crack width distribution remains unchanged over time. Crack width distribution showed no marked differences due to changes in ls values.

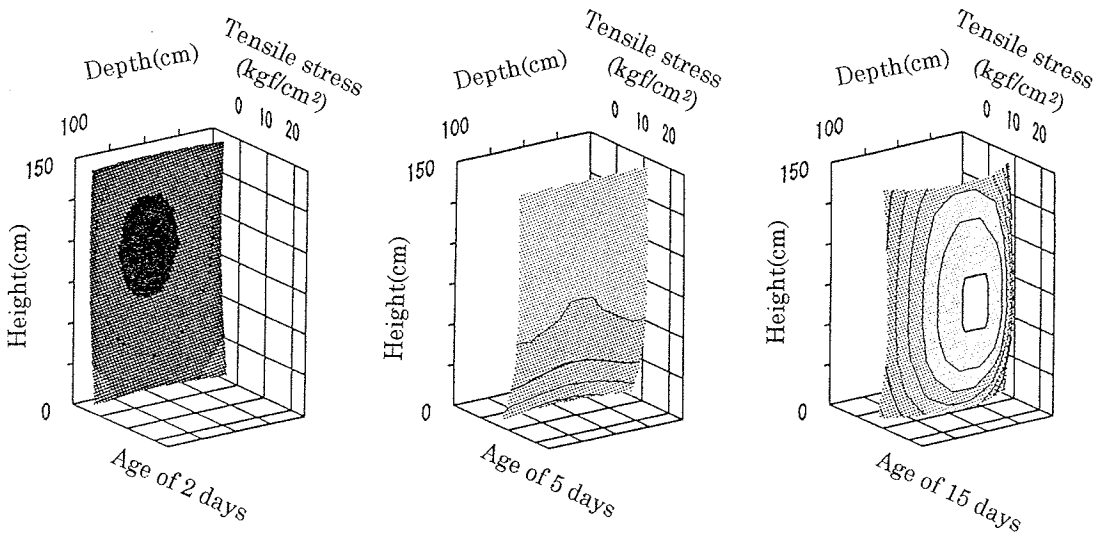

Fig. 15 3-D Distribution of Concrete Stress in the Wall

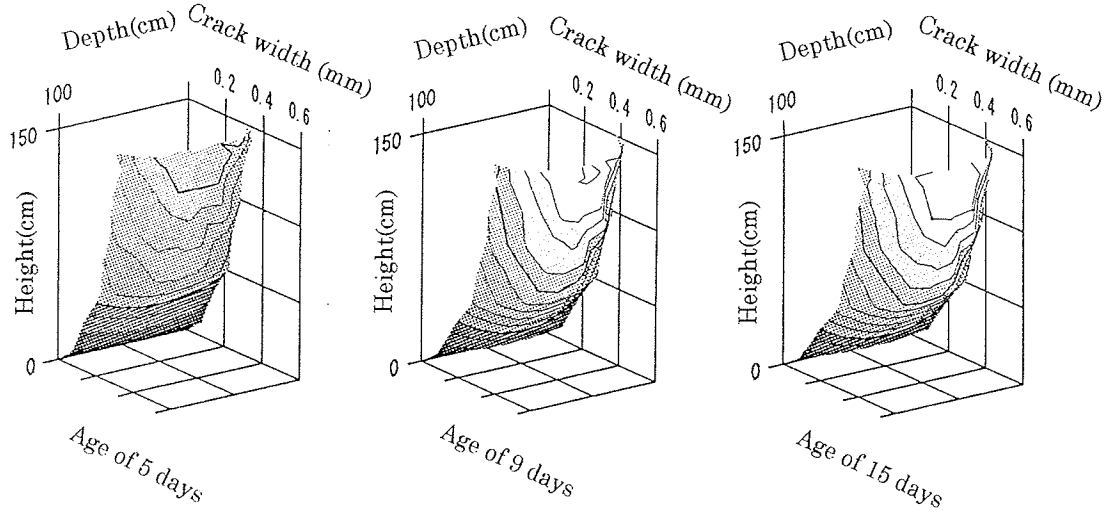

Fig. 16 3-D Distribution of Crack Width in the Wall

6.4 Applicability of 2-D analysis and extended CP method

a) Crack width

Figure 17 shows the crack width at the mid-level of the wall (Point C in Fig. 2) calculated by Case A (using average temperature) and Case B (using mid-thickness temperature) of the 2-D analysis in comparison with the measurements and calculations from the 3-D analysis. The shaded zone in the figure indicates the range between the crack widths at mid-thickness and on the surface from the 3-D analysis. In the 3-D analysis in this section, ls is assumed to be 15 cm. When comparing Case A and Case B of the 2-D analysis, Case B leads to larger crack widths by approximately 0.1 mm. When compared with actual measurements, both Case A and Case B crack width estimates are excessively small. The values calculated by Case B agree well with actual measurements immediately after cracking, but the difference between them tends to increase over time. In any event, the 2-D analysis tends to estimate crack widths as smaller than actual measured widths. It is therefore necessary to review the ls value and temperature distribution along the wall thickness, in other words, to investigate the effects of internally restrained stress and determine practical solutions for them. When compared with the 3-D analysis, both Case A and B of the 2-D analysis led to smaller calculated crack widths than even the surface crack widths by 3-D analysis. Figure 18 shows the calculations for the mid-height (Point C in Fig. 2) of the wall by extended CP method. The figure reveals that the extended CP method leads to crack widths larger than actual measurements by a maximum of 0.15 mm, but show fair congruence with the actual measurements as a whole. When comparing the extended CP method and the 3-D analysis, both show congruence throughout. Crack widths obtained by the extended CP method are larger than the surface crack widths from the 3-D analysis, and are instead closer to the mid-thickness values by the 3-D analysis. This is partly because the 3-D analysis assumes that the wall is perfectly bonded with the base, whereas the extended CP method assumes that separation occurs in the stress release zones.

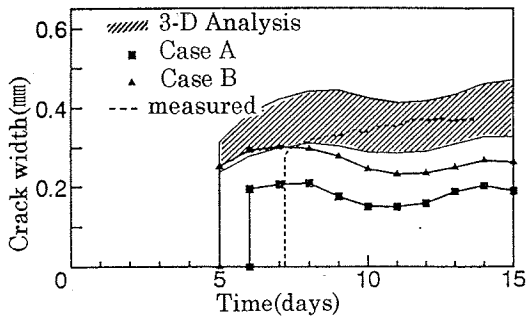

Fig. 17 Development of Crack Width(ls=15 cm) (Mid-height of the wall)

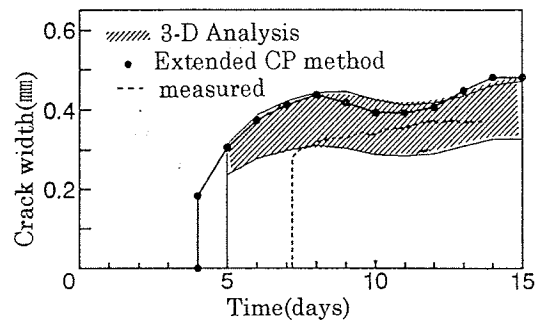

Fig. 18 Development of Crack Width(ls=15 cm) (Mid-height of the wall)

b) Reinforcement stress

Figures 19 and 20 show the reinforcement stress calculations by the 2-D analysis and extended CP method, respectively, at the position of the crack (Point B in Fig. 2). Figure 19 reveals that, similar to the crack width, the calculations by Case B (mid-thickness temperature) of the 2-D analysis agree well with the measurements immediately after cracking, but gradually become lower than the measurements over time. When compared with 3-D analysis, 2-D analysis generally leads to lower calculations with the exception of immediately after cracking. According to Fig. 20, the calculations by extended CP method are slightly lower than actual measurements and those by 3-D analysis, but tend to gradually increase and exceed them over time.

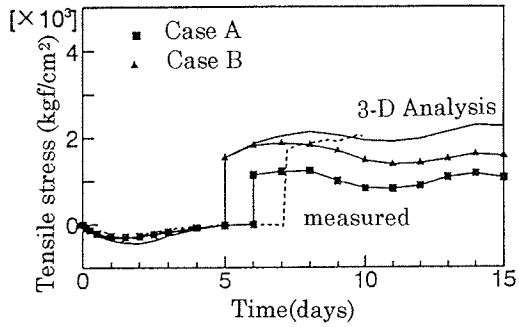

Fig. 19 Development of Reinforcement Stress (ls=15 cm)

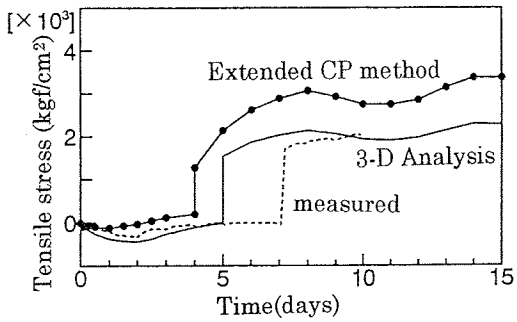

Fig. 20 Development of Reinforcement Stress (ls=15 cm)

c) Concrete stress

Figure 21 shows the calculations of concrete stress at the wall's mid-height (Point A in Fig. 2) of a section 2 m away from the crack calculated by the 2-D analysis. Figure 22 shows the calculations by extended CP method at the crack position, as this method's calculation program only outputs values for the crack position. The actual measurements are not shown in the figure, as the concrete stress at the crack position was not measured.

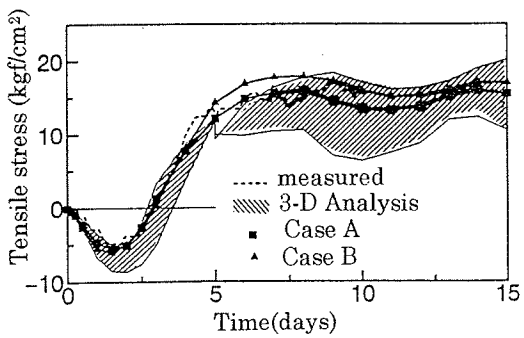

Fig. 21 Development of Concrete Stress (ls=15 cm)

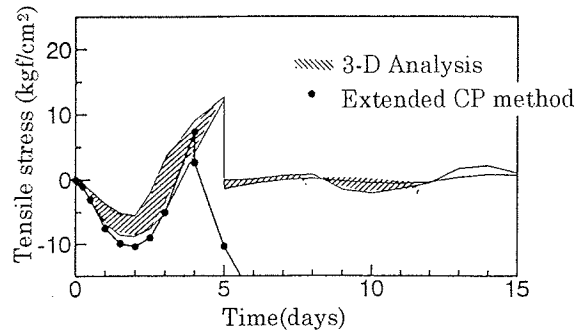

Fig. 22 Development of Concrete Stress (ls=15 cm)

Figure 21 reveals that both Case A and B of the 2-D analysis agree well with the actual measurements. Case B leads to approximately 10% higher stresses than Case A. The calculations by Case B agree relatively well with the mid-thickness stress values calculated by the 3-D analysis. Figure 22 reveals that the extended CP method leads to slightly higher values than the 3-D analysis. It should be noted that each method indicates the stress release at the time of cracking.

6.5 Crack width controlling effect of reinforcement

Figure 23 shows 3-D distribution of the crack width at 9 days with the reinforcement ratio being 0.27%, 0.6%, and 0.9%. The figure reveals that crack width is reduced over the entire section with an increase in reinforcement. No marked change is observed between the contours of crack width distribution with different reinforcement ratios. Figure 24 compares the vertical changes in the crack width on the surface between the different reinforcement ratios. As indicated in the figure, the crack width controlling effect of reinforcement shows a slight decrease as the reinforcement ratio increases.

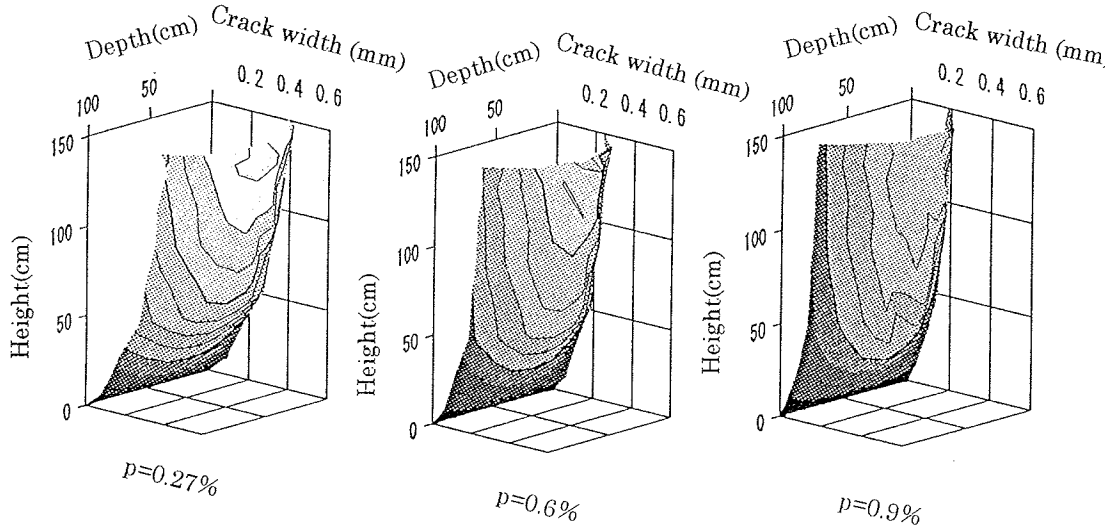

p: reinforcement ratio

Fig. 23 Crack Width Controlling Effect of Reinforcement

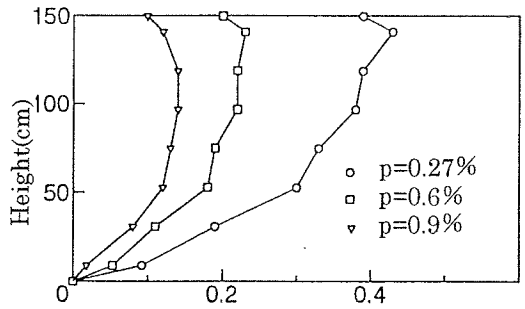

Fig. 24 Vertical Changes of Crack Width on the Surface

However, the maximum crack width is reduced to 58% and 40% when the reinforcement ratio is increased to 0.6% and 0.9%, respectively, when compared with the reinforcement ratio of 0.27%. In other words, according to the results of this analysis, the maximum crack width is 0.47 mm when the distributing bar ratio is 0.27%, which is normal practice; but the maximum crack width can be limited to under 0.2 mm by placing distributing bars at a reinforcement ratio of 0.6% or more. Adequate amount of reinforcement based on sufficient preliminary investigation makes the effective control of crack width possible.

7. CONCLUSIONS

In this study, the authors elucidated the 3-D distribution of thermal stress and crack width using the FEM into which a 3-D crack analysis model is incorporated. The investigation covered the optimum characteristic value, ls, of the analysis model, applicability of 2-D analysis and extended CP method, and the crack width controlling effect of reinforcement. The results obtained in this study are summarized as follows:

(1) Thermal crack width, concrete stress, and reinforcement stress can be estimated accurately by using a 3-D crack width analysis model. The characteristic value of the analysis model, ls, strongly affects the calculations of crack width and reinforcement stress. The optimum characteristic ls value is 15 to 20 cm.

(2) The distribution of thermal crack width in the wall forms a contour convex towards the upper center having the peak at mid-thickness near the top of the wall. The distribution contour remains unchanged with time. The ls value has no affect on the contour. The contour of concrete stress distribution changes from concave to convex with time.

(3) Two-dimensional analysis leads to low values of crack width and reinforcement stress compared with actual measurements or 3-D analysis. Particularly the effects of internal restraining stress should therefore be taken into account in the 2-D analysis. In regard to concrete stress, 2-D analysis values agreed relatively well with actual measurements and the mid-thickness stress calculated by 3-D analysis. The extended CP analysis led to slightly higher values of the crack width, reinforcement stress, and concrete stress than actual measurements or 3-D analysis.

(4) An adequate amount of reinforcement effectively controls the crack width. As the reinforcement content increases, the crack width is reduced over the entire wall section.

According to the analysis of this study, a reinforcement ratio of over 0.6% is required to effectively control the crack width.

References

[1] JCI committee on Thermal Stress of Massive Concrete Structure, " A Proposal of a Method of Calculating Crack Width Due to Thermal Stress", JCI Committee Report, 1992

[2] Kagohashi, H., Morimoto, H. and Koyanagi, W., " 3-Dimensinal Crack Analysis of Concrete Wall", Proc. of JCI, Vol. 16, No. 1, pp. 1359-1364, 1994 (in Japanese)

[3] Takai, S., Morimoto,H. and Koyanagi, W., " 3-Dimensinal Crack Analysis of Concrete Mass Concrete Structure", Proc. of JCI, Vol. 17, No. 1, pp. 1109-1114, 1995 (in Japanese)

[4] JCI Committee for Research and Study on Concrete Cracking, " Recommendation for Control of Cracking in Massive Concrete", JCI, pp. 127-160, 1986 (in Japanese)

[5] JCI Committee on Thermal Stress of Massive Concrete Structures, "State of the Art Report on Method of Calculating Thermal Stress of Mass Concrete", JCI, pp. 26-27,1985(in Japanese)

[6] Karino, T., Watanabe, H. and Khono, H., "Tensile Strength Characteristics of Concrete for Evaluation of Thermal Cracking", Annual Meeting of JSCE, Vol. 50, No. 5, pp. 732-733, 1995 (in Japanese)

[7] JCI, "Computer Program for Calculating Temperature, Stress and Crack width of Massive Concrete", 1993

[8] JSCE, "Standard Specification for Design and Construction for Concrete Structures (Part II Construction)", 1993